

# Universality in low energy states: from few-atoms to few-nucleons

A. Kievsky

*Istituto Nazionale di Fisica Nucleare, Largo Pontecorvo 3, 56100 Pisa, Italy*

M. Gattobigio

*Université de Nice-Sophia Antipolis, Institut Non-Linéaire de Nice,  
CNRS, 1361 route des Lucioles, 06560 Valbonne, France*

We investigate universal behavior in elastic atom-dimer scattering below the dimer breakup threshold calculating the atom-dimer effective-range function  $ak \cot \delta$ . We compare our results with the universal zero-range form deduced by Efimov,  $ak \cot \delta = c_1(ka) + c_2(ka) \cot[s_0 \ln(a\kappa_*) + \phi(ka)]$ , for different values of the two-body scattering length  $a$  and of the three-body parameter  $\kappa_*$ . We observe a good agreement introducing a particular type of finite-range corrections. Furthermore, we show that the same parameterization describes a very different system: nucleon-deuteron scattering below the deuteron breakup threshold. Our analysis reveals a universal behavior that ranges from few-atom systems to few-nucleon systems, and clarifies the nature of the pole structure in the effective-range function of nucleon-deuteron scattering.

*Introduction.* Scattering of two particles at very low energy shows universal behavior encoded in the scattering length  $a$  and in the effective range  $r_s$ . In fact, systems with different interactions sharing the same scattering length and the same effective range have the same effective range function,  $k \cot \delta = -1/a + r_s k^2/2$ , and, accordingly, the same low energy behavior. In the limit  $a \gg r_0$ , where the scattering length is much greater than the typical range  $r_0$  of the potential, not only the scattering process is universal, but also some bound-state properties. In fact, when  $a \rightarrow +\infty$  (known as unitary limit), the two-particle system has a shallow-bound state with the bound-state energy  $E_2 \approx \hbar^2/ma^2$  fixed by the scattering length. In this limit, the physics is scale invariant.

In the 1970s, V. Efimov [1, 2] showed that the scale invariance is broken in the  $s$ -wave three-body sector of a bosonic system. The residual symmetry is the discrete scale invariance (DSI); namely, the physics is invariant under the rescaling  $r \rightarrow \Lambda^n r$ , where the constant is usually written  $\Lambda = e^{\pi/s_0}$ , with  $s_0 \approx 1.00624$  an universal number that characterizes a system of three-identical bosons. One consequence is that at the unitary limit the three-body spectrum consists of an infinite number of states that accumulate to zero with the ratio between two consecutive states being  $E_3^{n+1}/E_3^n = e^{-2\pi/s_0}$ . For finite scattering length, the binding energies satisfy the Efimov's equation

$$E_3^n + \frac{\hbar^2}{ma^2} = e^{-2n\pi/s_0} \exp[\Delta(\xi)/s_0] \frac{\hbar^2 \kappa_*^2}{m}, \quad (1)$$

with  $\tan \xi = -(mE_3^n/\hbar^2)^{1/2}a$ . The function  $\Delta(\xi)$  is universal and a parameterization in the interval  $[-\pi, -\pi/4]$  is given in Ref. [3]. The three-body parameter  $\kappa_*$  is the wave number of the  $n = 0$  state at the unitary limit.

The DSI constrains the form of the observables to be log-periodic functions of the control parameters. One example is the atom-dimer scattering length which has

the general form

$$a_{AD}/a = d_1 + d_2 \tan[s_0 \ln(a\kappa_*) + d_3], \quad (2)$$

where  $d_1, d_2, d_3$  are universal constants to be determined. For collisions below the dimer breakup threshold, DSI imposes the following universal form for the effective range function

$$ka \cot \delta = c_1(ka) + c_2(ka) \cot[s_0 \ln(a\kappa_*) + \phi(ka)] \quad (3)$$

with  $\delta$  the atom-dimer phase-shift and  $c_1, c_2, \phi$  universal functions of the dimensionless variable  $ka$ , where  $k^2 = (4/3)E/(\hbar^2/m)$ , being  $E$  the center of mass energy of the process. As  $k \rightarrow 0$ ,  $ka \cot \delta \rightarrow -a/a_{AD}$  and at  $k = 0$  the constants  $d_1, d_2, d_3$  and  $c_1(0), c_2(0), \phi(0)$  are related by simple trigonometric relations.

In this paper we study in detail the universal behavior of  $a_{AD}$  and of the effective range function  $ka \cot \delta$ . To this aim we use the family of atomic  $^4\text{He}$ - $^4\text{He}$  potentials derived in Ref. [4] for several values of  $a$ , running from  $a \approx 440$  a.u. to  $a \approx 50$  a.u.. The corresponding dimer energies range from  $E_2 \approx 0.22$  mK to  $E_2 \approx 21$  mK covering two order of magnitude. For selected values of  $a$  in the mentioned interval we calculate  $a_{AD}$  and the  $s$ -wave phase-shifts in order to construct the effective range function below the dimer breakup threshold.

Our numerical results are used to analyze the universal form of Eqs. (2) and (3). As the value of  $a$  increases we observe that  $a_{AD}$  changes sign tending to  $-\infty$ . This behavior produces a pole in the effective range function. Furthermore, as the calculations are done using finite-range interactions, we can extract finite-range corrections by comparing our results to the zero-range theory. Interestingly, for the explored zone of positive scattering length, the range corrections can be taken into account by a shift in the variable  $\kappa_* a$ .

Finally, the universal character of the effective range function can be used to evaluate a very different system: low energy nucleon-deuteron scattering. It is well

known that the nucleon-deuteron effective range function presents a pole structure that has been related to the presence of a virtual state [5]. We shown that this structure is related to the universal form given by Eq.(3) and, using the parameterization determined in the atomic three-helium system, we shown that this equation can be used to describe nucleon-deuteron scattering as well. In this way, the universal behavior imposed by the DSI is analyzed in systems with natural lengths that differ of several order of magnitude.

*The three-boson model.* We construct the model using the LM2M2 [6], one of the most used  ${}^4\text{He}$ - ${}^4\text{He}$  potentials, as the reference interaction, with the mass parameter  $\hbar^2/m = 43.281307$  (a.u.)<sup>2</sup> K. Following Ref. [4] we define an attractive two-body Gaussian (TBG) potential

$$V(r) = V_0 e^{-r^2/r_0^2}, \quad (4)$$

with range  $r_0 = 10$  a.u. and strength  $V_0$  fixed to reproduce the values of  $a$  given by  $V_\lambda(r) = \lambda \cdot V_{\text{LM2M2}}(r)$ . The unitary limit appears at  $\lambda \approx 0.9743$  whereas for  $\lambda = 1$  the values of the LM2M2 are recovered:  $a = 189.41$  a.u.,  $E_2 = -1.303$  mK and  $r_e = 13.845$  a.u..

The use of the TBG potential in the three-atom system produces a ground state binding energy appreciable deeper than the one calculated with  $V_\lambda(r)$ . For example, at  $\lambda = 1$  the LM2M2 helium trimer ground state binding energy is  $E_3^0 = 126.4$  mK whereas the one obtained using the two-body-soft-core potential in Eq. (4) is 151.32 mK. Hence, we introduce a repulsive hypercentral-three-body (H3B) interaction

$$W(\rho_{123}) = W_0 e^{-\rho_{123}^2/\rho_0^2}, \quad (5)$$

with the strength  $W_0$  tuned to reproduce the trimer energy  $E_3^0$  obtained with  $V_\lambda(r)$  for all the explored values of  $\lambda$ . Here  $\rho_{123}^2 = \frac{2}{3}(r_{12}^2 + r_{23}^2 + r_{31}^2)$  is the hyperradius of three particles and  $\rho_0$  gives the range of the three-body force. Following Ref [4] we use  $\rho_0 = r_0$ .

Varying  $\lambda$  from the unitary limit to  $\lambda = 1.1$  we obtain a set of values for the ground state binding energy  $E_3^0$  and first excited state  $E_3^1$  using the TBG and TBG+H3B potentials in a broad interval of  $a$ . We can use the results for  $E_3^1$  at the unitary limit (using Eq.(1)) to determine  $\kappa_* = 0.002119$  a.u. and  $\kappa_* = 0.001899$  a.u. for the TBG and TBG+H3B, respectively. In Fig. 1 we collect our results for the ratio  $E_3^1/E_2$  as a function of  $\kappa_*a$  for the TBG potential (circles) and of the TBG+H3B potential (squares). We can compare the numerical predictions to the predictions of the Efimov's binding energy equations of Eq.(1), given in the figure by the dashed line. We can observe that the numerical results lie on a curve shifted with respect to the dashed line. We can interpret the shift as a consequence of the finite-range character of the numerical results. Accordingly, we can adapt the Efimov's equation to treat finite-range interactions. Once we fix  $n = 0$  for the first excited state  $E_3^1$ , we rewrite Eq. (1) as follow

$$E_3^1/E_2 = \tan^2 \xi, \quad \kappa_*'a = \exp[-\Delta(\xi)/2s_0]/\cos \xi, \quad (6)$$

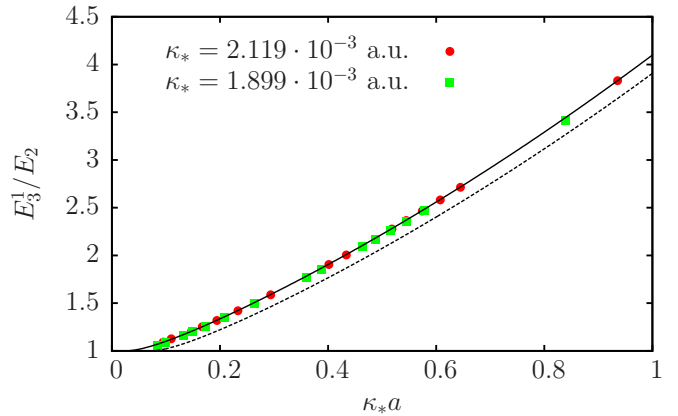


FIG. 1. (Color online) Energy of the first excited state of the trimer as a function of  $\kappa_*a$ . The dashed line is the universal prediction of the Efimov law, while the solid line is the translated universal curve. The circles and squares are the calculations using the TBG and TBG+H3B potentials respectively.

where we have introduced a finite-range three-body parameter

$$\kappa_*' \approx \kappa_*(1 + \epsilon + \dots), \quad (7)$$

with  $\epsilon = r_*/a$ . Therefore,  $\kappa_*$  and  $\kappa_*'$  are equal at the unitary limit ( $a \rightarrow \infty$ ) or in a zero-range theory ( $r_* \rightarrow 0$ ). In fact, the usual form of the Efimov's equations is recovered in both limits where  $E_2$  goes to zero (unitary limit) or  $E_2 \rightarrow \hbar^2/ma^2$  (the zero-range limit). In the present analysis we find  $r_* = 21$  a.u.  $\approx 2r_0$ . The corresponding results, obtained by solving Eq. (6) with  $\kappa_*' = \kappa_*a + \kappa_*r_*$ , are shown in Fig. 1 as a solid line.

*atom-dimer scattering.* To describe atom-dimer scattering below the dimer threshold we calculate  $a_{AD}$  and the  $s$ -wave atom-dimer phases  $\delta$  using the TBG and TBG+H3B potentials at different energies. We use the hyperspherical harmonic (HH) method in conjunction with the Kohn variational principle [7]. Applications of the method to describe a three-helium system with soft-core interactions as used here can be found in Ref. [8]. Defining  $E_2 = \hbar^2/ma_B^2$ , in Fig. 2 we show the results for the ratio  $a_{AD}/a_B$  in terms of the product  $\kappa_*a$ . It can be observed that the calculated points, given as full circles (TBG potential) and full squares (TBG+H3B potential), lie on a curve shifted with respect to the dashed line representing Eq.(2) with the parameterization of Ref. [3]. We can interpret again the shift as produced by the finite-range character of the calculations. Accordingly we can adapt Eq.(2) to describe finite-range interaction as

$$a_{AD}/a_B = d_1 + d_2 \tan[s_0 \ln(\kappa_*'a) + d_3]. \quad (8)$$

In fact, replacing in the above equation  $\kappa_*'a = \kappa_*a + \kappa_*r_*$ , with the same numerical value of  $r_*$  as before, the solid line is obtained in Fig. 2. The values  $d_1 = 1.531$

$d_2 = -2.141$ ,  $d_3 = 1.100$  slightly modify the parameterization of Ref. [3] to better describe the numerical results. This new parameterization is shown as a dotted line in the figure where we can observe an improvement in the description of the results close to the unitary limit.

The shifted formula can be used to determine the ratio  $a_*/a_-$ , where  $a_-$  is the scattering length at which the three-body states disappear into the three-atom continuum, and  $a_*$  is the scattering length at which the three-body states disappear into the atom-dimer continuum. For the potential models used in this work the values of  $a_-$  are given in Ref. [4] whereas the values of  $a_*$  can be extracted by equating the argument of the tangent in Eq.(8) to  $-\pi/2$ . Using these inputs we obtain  $a_*/a_- \approx -0.4$ . The zero-range universal formulas Eq. (1) and Eq. (2) predict  $a_*/a_- = -1.06$ , but recent experimental results give lower values for this ratio [9–11]; namely, it has been measured  $a_*/a_- \approx -0.7$  in potassium [9] and in bosonic lithium [11], while  $a_*/a_- \approx -0.4$  in cesium [10]. The difference is given by finite-range effects [12–16], which in our case are encoded in the shift.

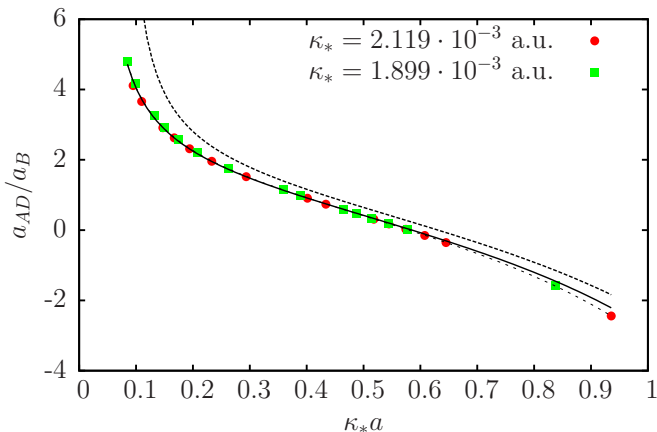


FIG. 2. (Color online) Universal plot for  $a_{AD}/a_B$  in terms of  $\kappa_* a$ . Open circles and open squares correspond to TBG and TBG+H3B potentials respectively. The dashed line corresponds to Eq. (2), whereas the solid line corresponds to Eq. (8). The dotted line shows the present parameterization of Eq. (8).

It is interesting to see that the finite-range corrections cancel in the description of the scattering length as a function of the trimer energy. This is shown in Fig. 3 in which the present calculations and the zero-range universal theory, Eqs. (1) and (2), are in close agreement.

We now present results for atom-dimer scattering at energies below the dimer breakup threshold for different values of  $a$ . We adapt Eq. (3) to finite-range interactions by considering  $ka_B \cot \delta$  as a function of the dimensionless center of mass energy  $(ka)^2$  and using  $\kappa'_* a = \kappa_* a + \kappa_* r_*$  in the argument of the logarithm func-

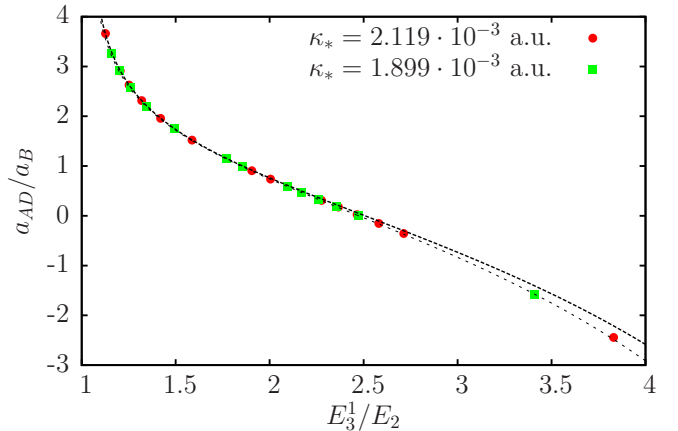


FIG. 3. (Color online) The ratio  $a_{AD}/a_B$  as a function of  $E_3^1/E_2$ . Open circles and open squares correspond to TBG and TBG+H3B potentials respectively. The dashed line corresponds to Eq. (2) with the parameterization of Ref. [3], whereas the dotted line shows the present parameterization of Eq. (8).

tion.

$$ka_B \cot \delta = c_1(ka) + c_2(ka) \cot[s_0 \ln(a\kappa'_*) + \phi(ka)]. \quad (9)$$

In Fig. 4 we show our results (given as full squares) at different values of  $\kappa'_* a$ . In the figure we can observe very different patterns. For the smallest values of  $\kappa'_* a$  the behavior is almost linear in all the energy range. Starting at values of  $\kappa'_* a \approx 0.4$  a curvature appears close to zero energy, pointing out to an emergent pole structure that becomes evident at larger values of  $\kappa'_* a$ . Specifically, the pole appears when  $a_{AD}$  changes sign (see Fig. 2) or, as given in Eq.(9), when the argument of the cotangent function becomes zero (or  $n\pi$ ). The shadow plot in the first row of Fig. 4 corresponds to the case  $\lambda = 1$  and describe  ${}^4\text{He}-{}^4\text{He}_2$  scattering (full triangles). The shadow plot in the second row corresponds to nucleon-deuteron scattering as discussed below. The solid curves are obtained using the finite-range-adapted Eq.(9) with the parameterization of Ref. [3]. We can observe a noticeable agreement along the whole range of values.

*nucleon-deuteron scattering.* The universal effective range function has been determined using the TBG and the TBG+H3B potentials describing an atomic three-helium system. The universal character of the function allow us to apply it to describe a very different system: nucleon-deuteron ( $n-d$ ) scattering. To this aim we use the results of Ref. [5] in which  $n-d$  scattering has been described using a spin dependent central potential. In that reference they obtained  $a_{nd} = 0.71$  fm for the  $n-d$  scattering length, and the effective range function has been parameterized as

$$k \cot \delta = \frac{-\frac{1}{a_{nd}} + \frac{1}{2} r_s k^2}{1 + E_{c.m.}/E_p} \quad (10)$$

with  $E_p = -160$  keV and  $r_s \approx -127$  fm. The pole ap-

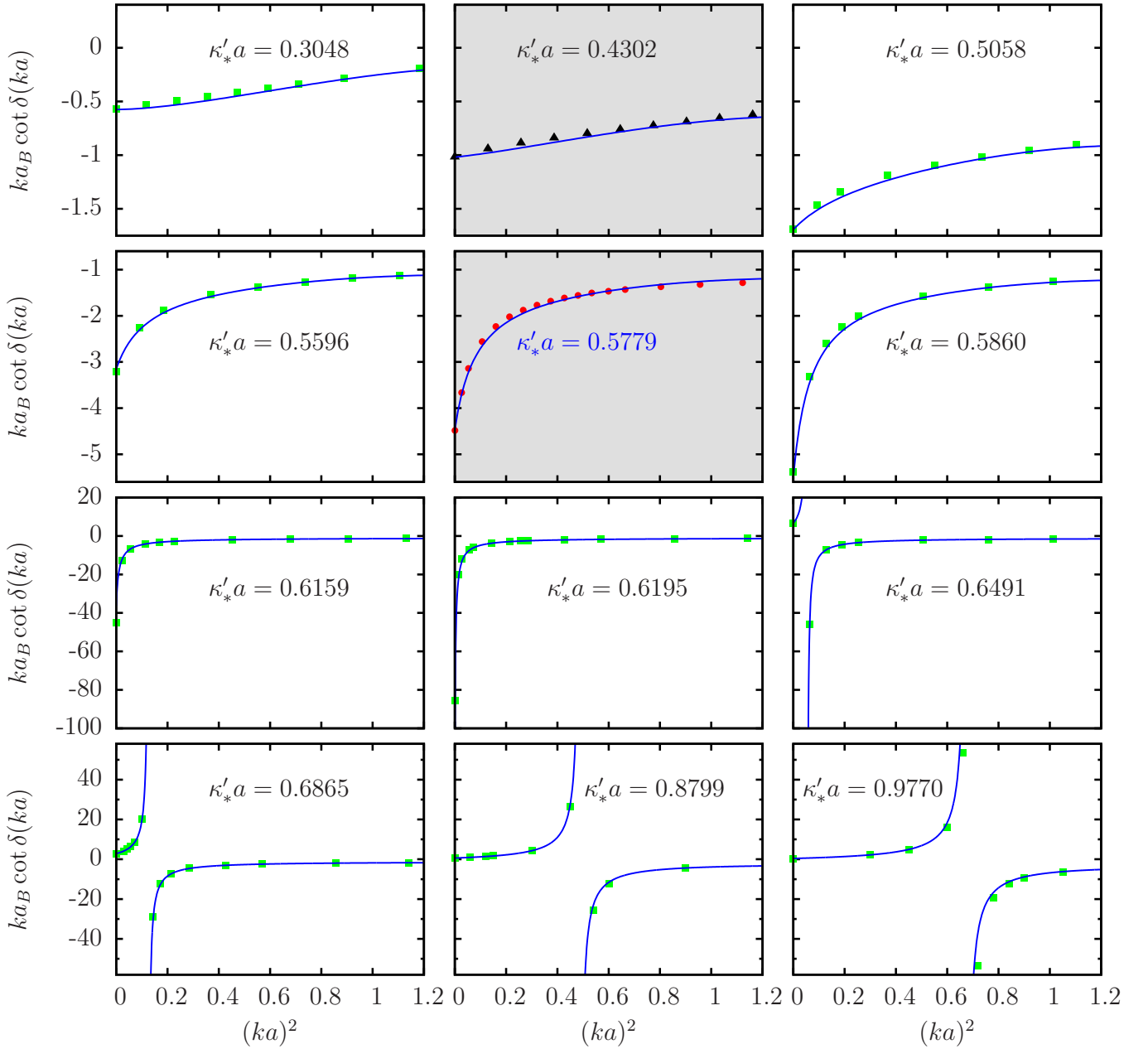


FIG. 4. (Color online) The effective range function at different values of  $\kappa_* a$  as a function of  $(ka)^2$ . The square points are our calculations; the triangle points are the calculations for real  ${}^4\text{He}$ - ${}^4\text{He}_2$  scattering. The full circles, for  $\kappa_* a = 0.543055$ , correspond to neutron-deuteron scattering in the doublet channel. The solid curves have been calculated using the translated-universal formula for the different values of  $\kappa_* a$ .

pears in the negative region similar to what happens in Fig. 4 at intermediate  $\kappa_*'a$  values. From the values of  $E_p$  and  $a_{nd}$  it is possible to determine the corresponding values of  $a$  and  $\kappa_*'$  by using the universal function  $\phi$  and Eq. (8). We obtain  $a = 4.075$  fm and  $\kappa_*'a = 0.5779$ . The shadow panel of the second row in Fig. 4 shows a comparison of the universal function (solid line) to the  $n-d$  scattering results of Ref. [5] (full circles). We observe a noticeable agreement. It should be noticed that the spin dependent potential used in Ref [5] reproduces the singlet

( ${}^1a_{np} \approx -20$  fm) and triplet ( ${}^3a_{np} \approx 5$  fm)  $n-p$  scattering lengths. Accordingly, the three-nucleon system has a symmetric plus a mixed symmetry component. The value of  $a$  extracted from the universal function, which is close to  ${}^3a_{np}$ , can be considered an effective value in an equivalent three-boson system with the given  $a_{nd}$  and the corresponding effective range function. A more deeper analysis extending the model to spin dependent interactions is at present underway.

In conclusion we have calculated the effective range

function in three-boson systems using the three-helium system as a reference. We have shown that the results can be described by the zero-range universal formula using a shifted three-body parameter  $\kappa'_*a = \kappa_*a + \kappa_*r_*$ . Interestingly, the value of  $r_*$  necessary to describe the results is the same for  $E_3^1$ , for  $a_{AD}$  and for the effective

range function. Furthermore, we used this function to describe low energy  $n - d$  scattering finding a quantitative agreement with calculations on this system. This analysis connects the universal behavior of atomic systems having large two-body scattering length to nuclear systems.

- 
- [1] V. Efimov, Phys. Lett. B **33**, 563 (1970).  
 [2] V. Efimov, Sov. J. Nucl. Phys. **12**, 589 (1971), [Yad. Fiz. **12**, 10801090 (1970)].  
 [3] E. Braaten and H. Hammer, Physics Reports **428**, 259 (2006).  
 [4] M. Gattobigio, A. Kievsky, and M. Viviani, Phys. Rev. A **86**, 042513 (2012).  
 [5] C. R. Chen, G. L. Payne, J. L. Friar, and B. F. Gibson, Phys. Rev. C **39**, 1261 (1989).  
 [6] R. A. Aziz and M. J. Slaman, J. Chem. Phys. **94**, 8047 (1991).  
 [7] A. Kievsky, Nuclear Physics A **624**, 125 (1997).  
 [8] A. Kievsky, E. Garrido, C. Romero-Redondo, and P. Barletta, Few-Body Syst. **51**, 259 (2011).  
 [9] M. Zaccanti, B. Deissler, C. D'Errico, M. Fattori, M. Jona-Lasinio, S. Müller, G. Roati, M. Inguscio, and G. Modugno, Nat Phys **5**, 586 (2009).  
 [10] F. Ferlaino, A. Zenesini, M. Berninger, B. Huang, H. C. Nägerl, and R. Grimm, Few-Body Syst. **51**, 113 (2011).  
 [11] O. Machtey, Z. Shotan, N. Gross, and L. Khaykovich, Phys. Rev. Lett. **108**, 210406 (2012).  
 [12] P. Naidon and M. Ueda, Comptes Rendus Physique **12**, 13 (2011).  
 [13] C. Ji, D. R. Phillips, and L. Platter, EPL **92**, 13003 (2010).  
 [14] J. P. D'Incao, C. H. Greene, and B. D. Esry, J. Phys. B **42**, 044016 (2009).  
 [15] M. Thøgersen, D. V. Fedorov, and A. S. Jensen, Phys. Rev. A **78**, 020501 (2008).  
 [16] T. Frederico, L. Tomio, A. Delfino, M. R. Hadizadeh, and M. T. Yamashita, Few-Body Syst. **51**, 87 (2011).